Dynamics of pedogenic carbonate growth in the tropical domain of Myanmar

A. Licht[1,2], J. Kelson[3], S. Bergel[2], A. Schauer[2], S.V. Petersen[3], A. Capirala[2], K.W Huntington[2], G. Dupont-Nivet[4,5], Zaw Win[6], and Day Wa Aung[7]

[1]Centre de Recherche et d'Enseignement de Géosciences de l'Environnement (CEREGE), Aix Marseille University, CNRS, IRD, INRAE, Aix-en-Provence, France

[2]Department of Earth and Space Sciences, University of Washington, Seattle, WA, USA

[3]Department of Earth and Environmental Sciences, University of Michigan, Ann Arbor, MI, USA

[4]Géosciences Rennes, CNRS and Université de Rennes 1, Rennes, France

[5]Institut für Geowissenschaften, Universität Potsdam, Potsdam, Germany

[6]Geology Department, Shwe Bo University, Sagaing Region, Myanmar

[7]Department of Geology, University of Yangon, Pyay Road, Yangon, Myanmar

Corresponding author: Alexis Licht (licht@cerege.fr)

Key Points:

- Tropical soil carbonates under monsoonal rainfall grow in winter and early spring.
- The cold-season bias in carbonate growth is promoted by warm (>15°C) winter temperatures and by high soil water content in summer and fall.
- Clumped isotope temperatures in tropical paleosols are likely impacted by changes of rainfall distribution.

This is the author manuscript accepted for publication and has undergone full peer review but has not been through the copyediting, typesetting, pagination and proofreading process, which may lead to differences between this version and the Version of Record. Please cite this article as doi: 10.1029/2021GC009929.

Abstract:

Pedogenic carbonate is widespread at mid latitudes where warm and dry conditions favor soil carbonate growth from spring to fall. The mechanisms and timing of pedogenic carbonate formation are more ambiguous in the tropical domain, where long periods of soil water saturation and high soil respiration enhance calcite dissolution. This paper provides stable carbon, oxygen and clumped isotope values from Quaternary and Miocene pedogenic carbonates in the tropical domain of Myanmar, in areas characterized by warm (>18°C) winters and annual rainfall up to 1700 mm. We show that carbonate growth in Myanmar is delayed to the driest and coldest months of the year by sustained monsoonal rainfall from mid spring to late fall. The range of isotopic variability in Quaternary pedogenic carbonates can be solely explained by temporal changes of carbonate growth within the dry season, from winter to early spring. We propose that high soil moisture year-round in the tropical domain narrows carbonate growth to the driest months and makes it particularly sensitive to the seasonal distribution of rainfall. This sensitivity is also enabled by high winter temperatures, allowing carbonate growth to occur outside the warmest months of the year. This high sensitivity is expected to be more prominent in the geological record during times with higher temperatures and greater expansion of the tropical realm. Clumped isotope temperatures, $\delta^{13}C$ and $\delta^{18}O$ values of tropical pedogenic carbonates are impacted by changes of both rainfall seasonality and surface temperatures; this sensitivity can potentially be used to track past tropical rainfall distribution.

Plain Language Summary

Soil carbonates are the focus of many continental paleoenvironmental studies because their isotopic composition records many features of the local environment (such as the type and density of vegetation, annual or warm season temperatures, and aridity). Soil carbonates are commonly studied in temperate and arid areas; in those environments, carbonates form during warm months when soils dry. Soil carbonates are rarer but present in the tropical domain, where their isotopic systematics and formation processes have been barely studied. This study provides stable isotopic data from soil carbonates in the tropical monsoonal domain of Myanmar, which is characterized by warm (>18°C), dry winters and abundant summer rainfall. We show that these soil carbonates grow during the coldest months of the year and follow different dynamics and isotope systematics than those of temperate and arid areas. We show that high soil wetness and warm temperatures year-round make carbonate growth particularly sensitive to the seasonal distribution of rainfall in the tropical domain. This seasonal sensitivity complicates the interpretation of soil isotopic data from past tropical ecosystems. We suggest that isotopic data from tropical paleoenvironments can be used as a proxy to reconstruct past rainfall distribution instead of average (or summer) environmental features.

1. Introduction

Soil carbonates are widespread from the low to high latitudes, today and in sedimentary archives, making them a valuable record of paleoenvironmental change through geologic time (e.g. Quade et al., 2011; Caves et al., 2015; Page et al., 2019; Xiong et al., 2020). However, most studies that investigate the features and

growth dynamics of modern pedogenic carbonates have focused on temperate and (semi-)arid soils at mid latitudes (Fig. 1), where calcic soils are abundant (e.g. Kelson et al., 2020). The isotopic systematics and dynamics of carbonate growth in modern tropical soils remain barely explored, and it is unclear when and how tropical carbonates grow.

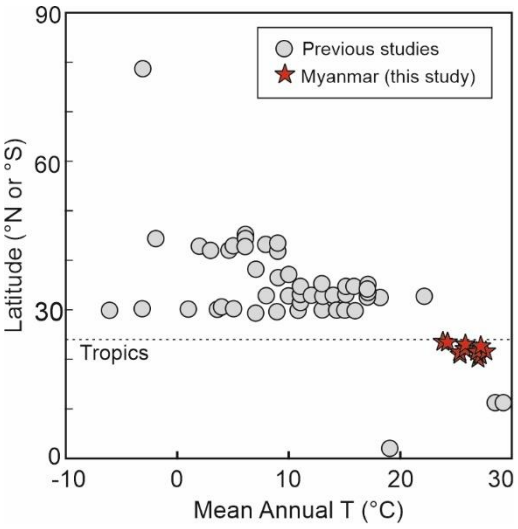

Figure 1. Mean annual temperature and latitude of clumped isotope data from this study and from previously studied sites with Holocene pedogenic carbonates (data screened for robustness by Kelson et al., 2020 --more than 2 replicates, sampling depth ≥40 cm).

Carbonate grows in soils where aqueous Ca^{2+} is available and usually undergoes multiple events of precipitation and dissolution that are controlled by soil water content, temperature, and CO_2 concentration on a yearly basis (Breecker et al., 2009; Huth et al., 2019); carbonate accumulates when long-term precipitation rates are higher than dissolution rates. Carbonate precipitation is favored during warm and dry times because high soil temperatures decrease calcite solubility while evaporation increases calcium activity in the soil water, and thus calcite saturation state (Gallagher and Sheldon, 2016; Fischer-Femal and Bowen, 2021). By contrast, carbonate dissolution is favored during wetter periods, especially during the plant growing season with high soil respiration and soil CO_2 maxima (Breecker et al., 2009). Soil carbonate growth temperatures reconstructed using clumped isotope thermometry ($T\Delta_{47}$) commonly show higher values than the Mean Annual air Temperature (MAT) in temperate and (semi-)arid ecosystems, supporting a warm-season bias in carbonate growth (Kelson et al., 2020). This warm bias relative to mean annual air temperatures is sometimes enhanced in arid and semi-arid environments (with commonly < 500 mm of annual rainfall): solar heating increases summer soil temperatures relative to air temperature where soil surface is bare, while winter snow cover can mute winter soil temperatures (Gallagher et al., 2019).

Pedogenic carbonates are rarer at low latitudes but can be found in tropical seasonal areas (areas with average monthly temperatures above 18 °C and at least one month with less than 60 mm of rainfall, sensu the Köppen classification), including close to the equator (Singh and Singh, 1972; Bettis et al., 2009). The mechanisms favoring soil carbonate formation and preservation in these warmer and wetter ecosystems are currently unclear given that higher soil respiration and longer periods of soil water saturation in tropical areas promote carbonate dissolution. In particular, the warm-season bias for carbonate growth may be less likely in the tropical domain with monsoonal rainfall as warm temperatures in the late spring and summer are associated with intense rainfall, soil water saturation, and high soil respiration. In some regions with seasonal summer rainfall outside the tropical domain, the carbonate growth season is delayed towards the fall such as in the Andes (Peters et al., 2013), but other regions such as Tibet do not show the same pattern (Quade et al., 2013; Burgener et al., 2018). A summer season bias for pedogenic carbonate growth remains the assumption

of most studies using bulk and clumped isotope proxies on paleosols, including in monsoonal Asia (Quade et al., 2011; Hoke et al., 2014; Ingalls et al., 2018; Botsyun et al., 2019; Xiong et al., 2020). This assumption is yet to be validated by a systematic study of soil carbonate growth in tropical climate.

We address this discrepancy by providing an expanded dataset of bulk and clumped isotope values from Quaternary and Miocene soil carbonates in the tropical domain of Myanmar, at sites where annual rainfall currently spans from 600 to 1700 mm. We show that our clumped and stable isotopic data indicate that carbonate growth varies locally from early winter to early spring. We explore the mechanisms leading to these cold-season $T\Delta_{47}$ values, unique so far in pedogenic carbonates, and highlight that soil carbonates grown under tropical climate may follow different clumped and stable isotope systematics from their temperate and arid counterparts.

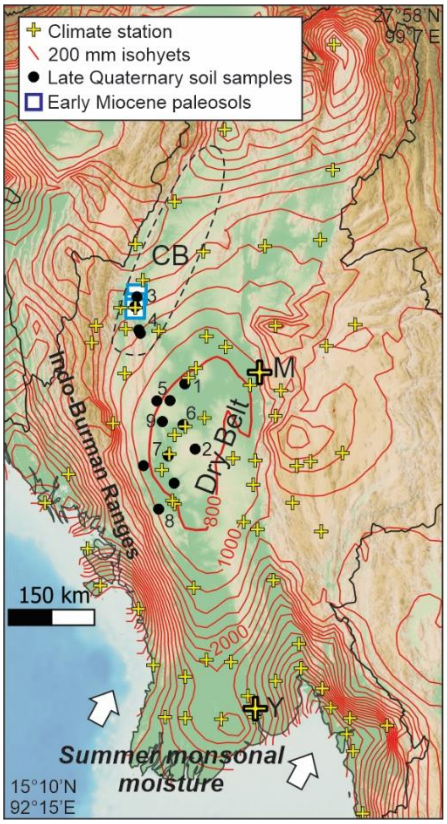

Figure 2. Map of western and central Myanmar with 200 mm isohyets of annual rainfall (red lines, from the WorldClim 2.1 model at 5 minutes spatial resolution; Fick and Hijmans, 2017), Burmese climate stations from the Burmese Department of Meteorology and Hydrology meteorological network (DMH; yellow crosses), Quaternary soil samples (black dots) and early Miocene paleosols (blue squares); numbers from 1 to 9 refer to sample location in Table 1. The location of the Mandalay (M) and Yangon (Y) climate stations (Fig. 3) is indicated with bold crosses. CB: Chindwin Basin (extent shown with dashed line).

2. Climate setting

Myanmar sits today in the South Asian monsoonal domain. Western Myanmar experiences intense summer rainfall (2-4 m from May to November) sourced from the Indian Ocean and amplified by the orographic effect of the Indo-Burman Ranges (Fig. 2). Lying in the rainshadow of the ranges, the central Myanmar lowlands are located near sea-level and experience dramatic changes of Mean Annual Precipitation (MAP) over short distances, from 4 m in southern Myanmar to 600 mm in the "dry belt" of central Myanmar. In contrast, the lowlands experience little spatial temperature variation in monthly temperatures (± 3°C of variation among climate stations). Most of central Myanmar lies within the Köppen tropical domain (i.e. areas with monthly average temperatures >18 °C): Mean Annual Temperature ranges from 23 to 28°C; winter monthly temperatures average 17 to 22°C, with minima of 10-15°C; average monthly temperatures peak at 30-33°C in April-May, with average monthly maxima of 40°C. Temperatures remain high (between 27 and 30°C) during the rainy season, which spans all summer and fall (Fig. 3a). The area is covered by mixed deciduous forests, woodlands, and savanna-woodlands. The vegetation is dominated by C3 trees and shrubs with limited herbaceous ground cover; C4 plants represent ca. 25% of the herbaceous vegetation (Khaing et al., 2019).

Unfortunately, there is no rainfall isotope data from the dry belt of central Myanmar. The closest GNIP station, Yangon, experiences more intense rainfall (> 2 m) and does not provide rainwater isotope data outside the monsoon season (Fig. 3b); New Delhi, India, receives a relatively low amount of annual precipitation (ca. 800 mm, mostly in JJA) and is the closest GNIP station with a similar monsoonal climate to the Burmese dry belt. Both stations display low $\delta^{18}O$ values through the monsoonal season, reaching their lowest $\delta^{18}O$ values (-8 to -9 ‰ VSMOW) in September (New Delhi) and October (Yangon). Non-monsoonal rainfall (December to May) in New Delhi is much more ^{18}O-enriched: -3 to +1 ‰ VSMOW, similar to what is seen regionally in South Asia (Araguas-Araguas et al., 1998). We assume the isotopic composition of rainfall in our study region to follow a similar seasonal pattern.

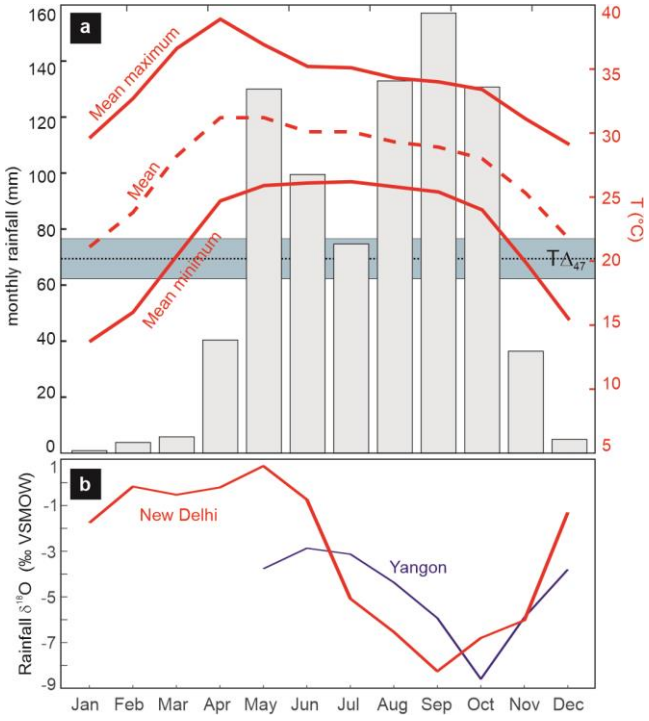

Figure 3. (a) Mean, mean maximum, and mean minimum monthly air temperatures (in red) and mean monthly precipitation (bars) in Mandalay (MAT: 27°C; MAP: 891 mm), displayed with the weighted average $T\Delta_{47}$ and standard error (2 SE) of all Burmese samples (in green). Mean temperature data are from the global historical climatology network monthly temperature dataset, version 4 (1961-2010; Menne et al., 2018); mean temperature maxima, minima, and rainfall data from the DMH network (1981-2010; Lai Lai Aung et al., 2017); Mandalay was chosen for display because it is the only climate station in central Myanmar that yields meteorological data from both the global historical climatology dataset and the DMH network. All climatic data are available in Supplementary Table 1. **(b)** Monthly rainfall $\delta^{18}O$ in Yangon (acquisition period: 1961-1963) and New Delhi (acquisition period: 1960-2012); data from the Global Network of Isotopes in Precipitation (GNIP); only May to December data are available in Yangon.

3. Methods

Our field investigations in central Myanmar show that pedogenic carbonates are widespread in the central dry belt and can be found in areas with up to 1.7 m of annual rainfall. We collected pedogenic carbonates from 15 localities at similar elevations along road cuts and badlands, in poorly developed soils (inceptisols) to ensure their young age. Three localities are soils developed on recent, loose river alluvium (including one on former farmland), and one locality on Mount Popa volcaniclastics attributed to the early Holocene (Belousov et al., 2018). The other localities are soils developed on tilted Eocene, Miocene and Pliocene sedimentary rocks; considering the recent deformation history of the central Myanmar lowlands (Plio-Pleistocene formation of regional anticlines; Pivnik et al., 1998) and the current high denudation rates in the

central dry belt during the monsoon season (Stamp, 1940), these soils are attributed to the Quaternary. Seasonal temperatures and rainfall amount at the 15 localities were obtained from three sources: 1) outputs from the WorldClim 2.1 model at 5 minutes spatial resolution (Fick and Hijmans, 2017); 2) variables from the closest climate station of the Burmese Department of Meteorology and Hydrology meteorological network (DMH) in central Myanmar (for monthly temperature maxima, minima, and rainfall amount; Fig. 2); and 3) variables at the locality extrapolated from all DMH climate stations with triangle-based cubic interpolation. The three approaches yield very similar results for monthly and annual variables (Supplementary Table 1).

Carbonate nodules were sampled at depths greater than 50 cm; up to five nodules per locality were selected for $\delta^{18}O$ and $\delta^{13}C$ analysis; samples were powdered and analyzed on a Kiel III Carbonate Device coupled to a Finnigan Delta Plus isotope ratio mass spectrometer at the University of Washington. Clumped isotope analysis was performed on one to two carbonate nodules from ten of the localities, with 4-11 replicates each; ten samples were analyzed at the University of Washington (digestion in a common acid bath held at 90 °C, purification on an off-line vacuum system, and analysis on a MAT 253, following Kelson et al., 2017) and at the University of Michigan (digestion and purification in a NuCarb automated sample preparation device held at 70 °C, and analysis on a Nu Perspective). The resulting Δ_{47} values are standardized to the InterCarb framework using carbonate reference materials ETH1, ETH2, ETH3, and ETH4 (Bernasconi et al., 2021). The uncertainty in the Δ_{47} values is reported as the standard error of the mean of replicate analyses for each carbonate sample. To calculate the standard error, we employed whichever is larger: the long-term standard deviation of a carbonate reference material (reference material information is listed in the supplementary material) or the standard deviation of the replicate analyses (see Kelson et al., 2020 for more details on the calculation). The Δ_{47} values are then converted to clumped isotope temperatures ($T\Delta_{47}$, in °C) following Anderson et al. (2021); soil water $\delta^{18}O$ is calculated from carbonate $T\Delta_{47}$ and $\delta^{18}O$ values using the calcite-water fractionation equation of Kim and O'Neil (1997).

We calculated soil CO_2 $\delta^{13}C$ isotopic composition at each site from their average carbonate $\delta^{13}C$ value, using the T-dependent fractionation equation of Romanek et al. (1992) and an estimate of soil temperature during carbonate growth. These estimates were obtained from either the $T\Delta_{47}$ value at the site if one measurement was made at the site (n=8), the average $T\Delta_{47}$ value if two measurements were made (n=3), or the average $T\Delta_{47}$ value at all localities (20.1 °C; see next section) if no clumped isotopic data were acquired (n=4). Finally, for eleven of the localities, we acquired solid organic matter $\delta^{13}C$ values from decarbonated material from the carbonate layers. Solid samples were left overnight with 6M HCl in an oven at 60-80°C and rinsed with DI water the following day, and thus for three consecutive days; $\delta^{13}C$ values of decarbonated material were acquired with a Costech Elemental Analyzer, Conflo III, MAT253 in continuous flow mode at the University of Washington.

We also sampled pedogenic nodules from the upper lower Miocene to lowermost middle Miocene Natma Formation in the Chindwin Basin, close to our wettest localities (modern MAP: ca. 1700 mm; Fig. 2). The Natma Formation consists of fluviatile deposits rich in paleosols (mostly cumulative argillisols and rare

argillic calcisols) and fossil wood specimens typical of moist deciduous to (semi-)evergreen forests found in monsoonal Southeast Asia (Gentis et al., 2019; Westerweel et al., 2020). Paleosols commonly lack an A horizon and the depth of their calcic Bk horizon is unknown; when possible, we sampled the deepest nodules of the Bk horizon. Thirty samples from seven localities were prepared in thin section and examined using polarized light microscopy to evaluate the absence of secondary, sparitic calcite. Nineteen of these pedogenic carbonate samples were analyzed for carbon and oxygen isotopes; two samples were almost devoid of sparite and selected for clumped isotope analysis at the University of Washington. We also acquired solid organic material $\delta^{13}C$ values from decarbonated material of the carbonate layers for four of the localities.

Location of samples, soil and paleosol details (sampling depth, soil texture and vegetation cover), and climate variables at the site and at the nearest climate stations are given in Supplementary Table 1; a synthesis of clumped isotope data is provided in Table 1; detailed bulk and clumped isotope results together with analytical procedures and details on reference material are given in Supplementary Table 2, and microphotographs of thin sections for diagenetic screening in Supplementary file 1. Raw clumped isotopic data from the University of Washington and University of Michigan are given in Supplementary Tables 3 and 4.

4. Results

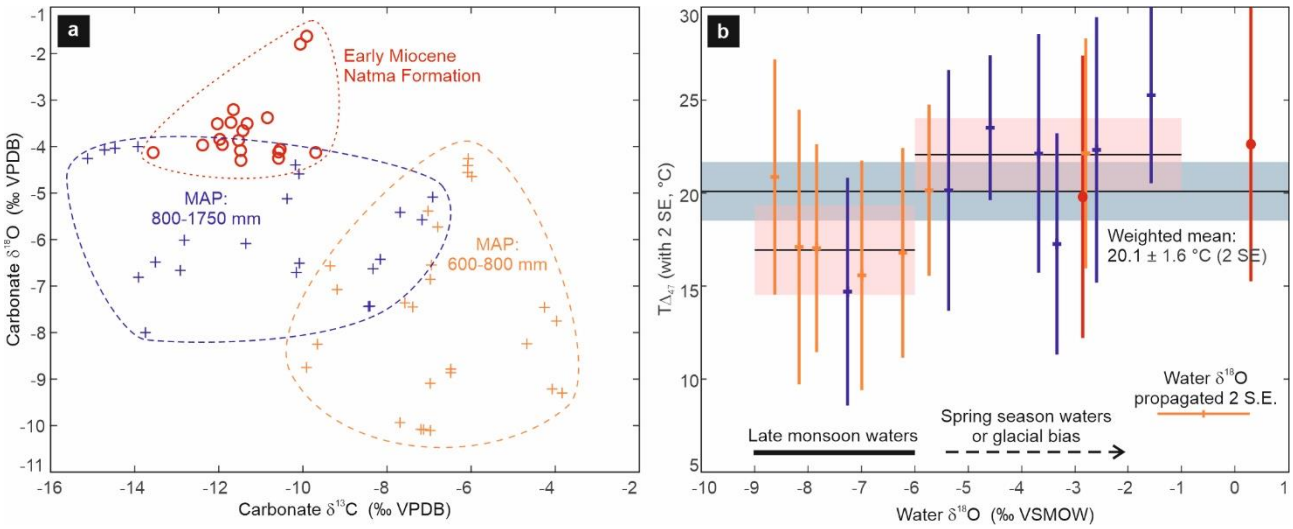

Figure 4. (a) Oxygen and carbon isotopic compositions of pedogenic carbonates from central Myanmar. Quaternary samples (crosses) are sorted following the MAP at their locality: 600-800 mm (in orange), 800-1750 mm (in blue); early Miocene samples (circles) are displayed in red. **(b)** $T\Delta_{47}$ values and water $\delta^{18}O$ values of pedogenic carbonates from central Myanmar (color coding same as in a); the weighted mean and weighted standard error (2 SE) are displayed in gray for all Quaternary samples and in pink for samples with water $\delta^{18}O$ values below and above 6 ‰. Error bars for $T\Delta_{47}$ values are 2 SE of replicate analyses. Propagated $T\Delta_{47}$ error in water $\delta^{18}O$ values (always <1.6 ‰ at 2 SE, see table 1) is not shown for every sample but its common width is illustrated (orange horizontal bar). The range of rainwater $\delta^{18}O$ values for the late monsoon season in the Bengal Bay is also displayed, together with the common values of spring season rainwaters; glacial $\delta^{18}O$ values are expected to be ca. 2 ‰ more enriched than today in the area (Liu

et al., 2020).

We split the dataset of Quaternary carbonates into two climatic groups of similar sample size for a balanced comparison: samples from localities below and above 800 mm MAP. Localities with MAP below 800 mm (7 localities, 26 stable isotopic and 7 clumped isotopic data points) cover a wide range of carbonate $\delta^{18}O$ values: from -4 to -10 ‰ VPDB, with an average of -7.6 ‰ (Fig. 4a). Carbonate $\delta^{13}C$ values range between -3 and -10 ‰ VPDB (average: -6.7 ‰). $T\Delta_{47}$ values range from 15 ± 6 °C to 22 ± 6 °C (2 SE), with a weighted average and standard error of 18.7 ± 2.2 °C (2 SE; Fig. 4b). Water $\delta^{18}O$ values reconstructed from $T\Delta_{47}$ and carbonate $\delta^{18}O$ values range from -3 to -9 ‰ VSMOW (average -6.6 ‰). In contrast, localities with MAP above 800 mm (8 localities, 22 stable isotopic and 7 clumped isotopic data points) display higher $\delta^{18}O$ values, spanning from -4 to -8 ‰ VPDB, with an average at -5.8 ‰. Carbonate $\delta^{13}C$ values are lower, from -7 to -14 ‰ VPDB (average: -11.0 ‰). $T\Delta_{47}$ values range from 15 ± 6 °C to 25 ± 5 °C (2 SE), with a weighted average and standard error of 21.4 ± 2.1 °C (2 SE). Water $\delta^{18}O$ values reconstructed from $T\Delta_{47}$ values range from -2 to -7 ‰ VSMOW (average -4.0 ‰). The weighted average $T\Delta_{47}$ value of both groups remains close to the weighted average of the complete population (20.1 ± 1.6 °C, 2 SE), and a t test using $T\Delta_{47}$ values indicate that the statistical difference between both groups is not significant ($p = 0.14$). Interestingly, samples with low water $\delta^{18}O$ values are almost systematically associated with lower-than-average $T\Delta_{47}$ values, while samples with high water $\delta^{18}O$ values are associated with the warmest temperatures. Carbonates with $\delta^{18}O$ values below -6 ‰ VSMOW (6 samples) have an average $T\Delta_{47}$ value of 16.9 ± 2.5 °C (2 SE), while samples with $\delta^{18}O$ values above -6 ‰ VSMOW (8 samples) have an average $T\Delta_{47}$ value of 22.0 ± 1.9 °C (2 SE). A t test using $T\Delta_{47}$ values finds that samples that have $\delta^{18}O$ values below and above -6 ‰ are statistically different ($p = 0.0014$) by 2-7 °C (95% confidence interval). Finally, soil organic matter sampled in the carbonate layers at eleven localities displays $\delta^{13}C$ values ranging from -27 to -22 ‰ VPDB (Fig. 5), with no clear difference between groups. These values are typical of the $\delta^{13}C$ range for C3 flora outside tropical rainforests (Kohn, 2010), but do not reject a potential presence of a small proportion of C4 plants (<20 %).

Samples from the Miocene Natma Formation (7 localities, 19 stable isotopic and 2 clumped isotopic data points) display carbonate $\delta^{18}O$ values between -3 to -5 ‰ VPDB (average: -3.6 ‰), with the exception of one locality that displays higher values (between -1 and -2 ‰). Carbonate $\delta^{13}C$ values range from -9 to -14 ‰ VPDB (average: -11.3 ‰). $T\Delta_{47}$ values equal 20 ± 8 °C and 23 ± 6 °C (2 SE), with reconstructed water $\delta^{18}O$ values from -3 to 0 ‰ VSMOW. Lastly, soil organic matter at four localities displays $\delta^{13}C$ values ranging from -26 to -24 ‰ VPDB, typical of C3 flora outside tropical rainforests (Fig. 5).

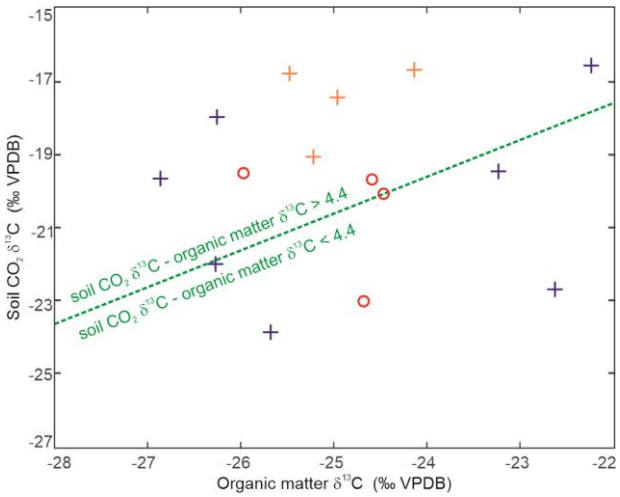

Figure 5. Organic matter $\delta^{13}C$ values for the Quaternary and Miocene localities, compared to their calculated soil CO_2 $\delta^{13}C$ values (see main text). Color coding is the same as Figure 4: Quaternary samples at localities with MAP < 800 mm (orange crosses), > 800 mm (blue crosses), and Miocene samples (red circles). The dashed green line highlights the domain where soil CO_2 $\delta^{13}C$ = organic matter $\delta^{13}C$ + 4.4 ‰, the minimum fractionation observed if soil carbonates and organic matter are contemporaneous (Cerling et al., 1991; Montanez, 2013).

Localities			Climate parameters from WorldClim V2, res: 5min				Clumped isotopic data										
age	location on fig. 1	name	MAT (in °C)	WMMT (in °C)	CMMT (in °C)	MAP (in mm)	*n*	Carbonate $\delta^{13}C$ (‰ VPDB)	$\delta^{13}C$ S.E. (‰)	Carbonate $\delta^{18}O$ (‰ VPDB)	$\delta^{18}O$ S.E. (‰)	Δ_{47} I-CDES25 (‰)	Δ_{47} S.E. (‰)	$T\Delta_{47}$ (°C)	$T\Delta_{47}$ S.E. (°C)	Soil Water $\delta^{18}O$ (‰ VSMOW)	Soil Water $\delta^{18}O$ propagated S.E. (‰)
Quaternary soils	1	17NOD01	27.2	31.3	21.2	747	8	-6.08	0.02	-4.56	0.16	0.6904	0.0092	22.1	3.0	-2.8	0.6
	2	17NOD04	25.1	29.6	19.9	772	11	-6.97	0.04	-10.11	0.02	0.6943	0.0099	20.9	3.2	-8.6	0.7
	3	19NOD02	24.3	28.5	18.1	1701	6	-10.18	0.02	-4.39	0.03	0.6898	0.0107	22.3	3.5	-2.6	0.7
	3	19NOD03	24.3	28.5	18.1	1701	7	-10.16	0.03	-6.71	0.07	0.6965	0.0099	20.2	3.1	-5.3	0.6
	4	19NOD04	25.7	29.8	19.5	1372	9	-14.72	0.01	-4.07	0.03	0.7056	0.0097	17.3	3.0	-3.3	0.6
							4	-13.92	0.01	-4.00	0.02	0.6806	0.0073	25.4	2.4	-1.5	0.5
	5	19NOD06	25.7	30.0	20.0	845	7	-8.44	0.02	-7.44	0.03	0.7140	0.0099	14.7	3.0	-7.2	0.6
							6	-8.33	0.01	-6.63	0.07	0.6862	0.0059	23.5	2.0	-4.6	0.4
	6	19NOD07	27.6	31.9	22.1	647	10	-6.97	0.01	-6.85	0.03	0.7072	0.0092	16.8	2.8	-6.2	0.6
	5	19NOD08	27	31.3	21.3	720	10	-6.48	0.02	-8.86	0.13	0.7061	0.0121	17.1	3.7	-8.1	0.8
	7	19NOD09	27.3	31.6	21.9	655	7	-7.57	0.06	-7.36	0.07	0.7111	0.0099	15.6	3.0	-7.0	0.6
	8	20NOD01	27	31.5	20.9	869	7	-7.70	0.09	-5.43	0.07	0.0096	0.0099	22.2	3.2	-3.6	0.7
	9	20NOD03	26.8	31.0	21.4	723	8	-9.89	0.02	-8.59	0.06	0.7063	0.0093	17.1	2.9	-7.9	0.6
							4	-9.19	0.01	-7.07	0.03	0.6965	0.0073	20.2	2.3	-5.7	0.5
Early Miocene	3	19NAT13	N/A				8	-9.70	0.48	-4.13	0.90	0.6976	0.0121	19.8	3.8	-2.8	0.8
	3	19NAT01	N/A				5	-9.91	0.06	-1.63	0.05	0.6881	0.0091	22.9	3.0	0.3	0.6

Table 1. Synthesis of clumped isotope data and soil water $\delta^{18}O$ at each locality; climatic parameters from Worldclim V2 at 5 minutes resolution; alternate climate parameters and soil morphology at every locality described in Supplementary Table 1, detailed clumped isotope data in supplementary Table 2. *n* = number of replicates. Δ_{47} values are normalized to the InterCarb Reference frame at 25 °C (I-CDES25, Bernasconi et al., 2021); $T\Delta_{47}$ values are calculated with a temperature-Δ_{47} relationship of Anderson et al. (2021). Soil water $\delta^{18}O$ values are calculated from carbonate $\delta^{18}O$ and $T\Delta_{47}$ values using the equation of Kim and O'Neil (1997). Propagated $T\Delta_{47}$ error in water $\delta^{18}O$ values range from 0.8 to 1.6 ‰ (2 SE).

5. Discussion

5.1 Cold season bias or a record of glacial periods?

The average $T\Delta_{47}$ value (20.1 ± 1.6 °C, 2 SE) is colder than the MAT at the study sites (24-28°C). This value is only reached today in central Myanmar during winter (DJF; Fig. 2). The $T\Delta_{47}$ values of some individual sites are colder on average than winter temperatures (15 ± 6 °C, 2 SE), but still overlap with the Coldest Month Mean Temperature (CMMT) at the study sites (17-22 °C). While we currently lack radiocarbon age constraints on our samples, this misfit suggests that these soil carbonates formed, or partially formed, during colder periods of the Quaternary.

Carbon isotopic data also support the idea that some of the soil carbonates at the wetter sites might have formed at least partially during an earlier period or might integrate over a longer period of time (> several millennia) with varying environmental conditions. Soil CO_2 has a carbon isotopic composition at least 4.4-4.2 ‰ higher than soil organic matter due to differences in diffusion between different CO_2 isotopologues during soil respiration (Cerling et al., 1991). Differences lower than 4.4-4.2 ‰ can be explained as related to recent changes in soil organic matter because labile organic matter has a faster turnover rate than pedogenic carbonate growth (Montanez, 2013). Of the wet sites (MAP > 800 mm) for which we have $\delta^{13}C$ values of organic matter, more than half (4 out of 7) display soil CO_2 $\delta^{13}C$ values that are less than 4.4 ‰ higher than those of the soil organic matter (Fig. 5). These results indicate that carbonates at the wettest sites grew partly (or completely) from soil-respired CO_2 and organic matter that was more ^{13}C-depleted than the modern soil organic matter, which supports an earlier origin during the Quaternary for some of our samples. Plant carbon isotopic composition in monsoonal (sub)tropical forests mainly relates to habitat openness, with lowest $\delta^{13}C$ values in areas with the lowest light availability (Ehleringer et al., 1987). At a broader spatial scale, plant carbon isotopic composition in C3 plant communities is linked to humidity, with lowest $\delta^{13}C$ values in the wettest areas (Kohn, 2010). Therefore, more ^{13}C-depleted soil-respired CO_2 at the time of carbonate formation at the wettest sites indicates that these carbonates grew at least partially under denser forest cover than is present today, and possibly wetter conditions.

Surface temperatures were ca. 2-5°C lower in South Asia during the last glacial maximum (Saraswat et al., 2013; Liu et al., 2020); partial carbonate growth during previous glacial periods could thus explain the colder-than-winter values found in some of our samples. However, it is difficult to assess if the more forested and possibly wetter conditions do indeed correspond to the last glacial periods, as the past hydrological history of Myanmar is poorly understood. Climate simulations suggest an increase of annual rainfall over the Indo-Burman Ranges and western Myanmar during the last glacial period (Di Nezio et al., 2018), corroborated by higher erosion rates in the ranges (Colin et al., 2001). In contrast, speleothems in eastern Myanmar (Shan-Thai Highlands) and Thailand suggest a ~60% decrease of monsoonal rainfall at that time (Liu et al., 2020). Human-mediated deforestation during the late Holocene also could have partly driven the observed discrepancy between carbonate and organic matter $\delta^{13}C$ values. The two Miocene samples analyzed here yield $T\Delta_{47}$ values (20 and 23 °C) similar to the weighted $T\Delta_{47}$ average of our Quaternary samples. The two soil localities unequivocally attributed to the Holocene (19NOD07, developed on former farmland, and 17NOD04, developed on early Holocene volcaniclastics) yield similar temperatures (17 and 21°C). This suggests that the integration of glacial temperatures in our Quaternary $T\Delta_{47}$ values is not the main driver lowering our carbonate growth temperature record to coolest average monthly temperatures.

When decreased by 2 to 5 °C, as expected for air temperatures during the last glacial period in South Asia, the average $T\Delta_{47}$ temperature (20.1 ± 1.6 °C, 2 SE) remains within the range of monthly average temperatures during winter to early spring (December to April; e.g. Fig. 3a). Our $T\Delta_{47}$ values thus indicate a cold-season bias in carbonate growth, even when considering a potential integration of soil temperatures through multiple glacial and interglacial cycles.

5.2 Presence, mechanisms and timing of carbonate growth in the tropical domain

The presence of soil carbonate in some of the wettest parts of central Myanmar, and their growth during possibly wetter conditions, is contrary to the traditional wisdom that soil carbonates do not form in environments with MAP > 1000 mm/year (Retallack, 2005). While this occurrence is rare, soil carbonates have been observed in "wet" localities such as northern India (Singh and Singh, 1972) and Tennessee, USA (Railsback, 2021). Quaternary pedogenic nodules are also found in multiple localities near the equator in Java (latitude ca. 7°N), in areas with prominent seasonality and modern annual rainfall exceeding 1700 mm (van Der Kaars and Dam, 1997; Bettis et al., 2009). Following Breecker et al. (2009, 2010), we propose that the intensely seasonal nature of precipitation and soil water content in Myanmar allows for preferential formation of carbonates during the dry season, in winter and early spring.

The long monsoonal season in Myanmar, with intense and steady rainfall from May until October (Fig. 3a), results in a delayed peak of soil moisture in late Fall (mid November; Fig. 6). In winter and spring (December to May), central Myanmar experiences little rainfall and monthly temperatures remain above 15°C; these warm and dry conditions allow the soils to steadily dry until the onset of the next monsoon season. Pedogenic carbonates in this region are thus expected to form throughout the winter and spring, including through the spring months of April and May when monthly temperatures peak above 30°C, as soil drying continues to concentrate Ca^{2+} ions in the soil and promote saturation of calcite (Breecker et al., 2009). Our $T\Delta_{47}$ values do indeed indicate that carbonate growth occurs here in the dry season, but display an apparent bias towards the early winter, i.e. the earliest part of the dry season. This bias could partly result from an imprint of glacial temperatures, or alternatively suggests a narrow period of carbonate growth at the start of the seasonal dewatering phase. Specifically, this apparent bias in temperatures could be a result of two processes: 1) soil respiration may increase enough in late spring to reduce calcite precipitation and/or 2) carbonate that forms in later spring may be more sensitive to dissolution than winter-grown carbonates, as described in the following paragraphs.

(1) Soil respiration is primarily controlled by soil moisture in Asian monsoonal ecosystems, with low values in the dry season and high values during the monsoon season (Kume et al., 2013, Hanpattanakit et al., 2015). Winter months in central Myanmar display the lowest monthly rainfall amount (commonly <10 mm per month from December to March; Fig. 3a). Sparse but heavy rain events during mid-spring (April-May) do not impact the average soil moisture budget (Fig. 6) but could result in rain-induced soil respiration pulses, as seen in other seasonal tropical forests (Rubio and Detto, 2017). These pulses of soil moisture and soil respiration could prevent spring carbonate growth. In addition to this important moisture control, temperature variations within the dry season sometimes secondarily impact soil respiration (Meena et al., 2020) and thus

the timing of carbonate growth. In this setting, mild temperatures (warmer than usual for cold regions, but colder than usual for warm regions) in December and January could drive down soil respiration, reducing soil CO_2 concentrations and favoring carbonate growth.

(2) Pedogenic carbonate that forms in late spring might not preserve as easily as carbonate forming in winter. Late spring rain events or summer monsoonal rainfall could preferentially dissolve freshly-grown carbonates and/or the outermost layers of older carbonates, leaving behind only the remnants of early, winter-grown carbonates. The mechanisms for this potential bias in dissolution remain unclear, but could relate to varying texture and/or soil depth between carbonates grown at different times of year.

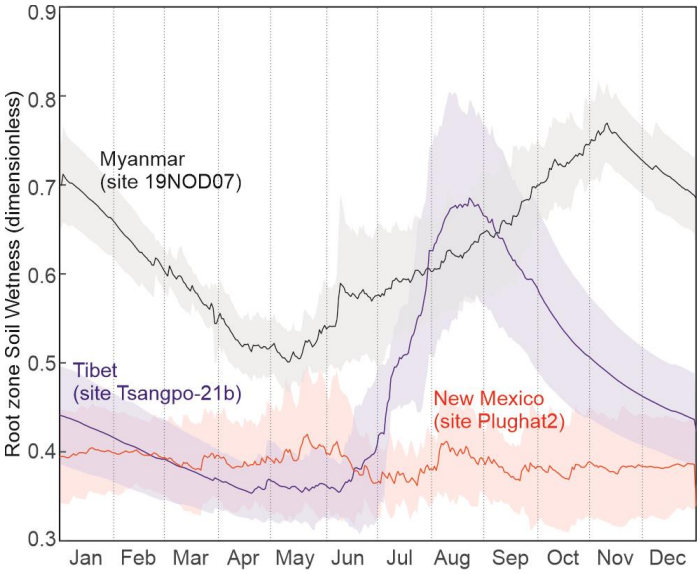

Figure 6. Root zone (0-100 cm) soil wetness from SMAP L4 satellite data averaged over the years 1979-2008 (Reichle et al., 2018) at three sites with pedogenic carbonate clumped isotope data: Tsangpo-21b in Tibet (in blue; Burgener et al., 2018), Plughat-2 in New Mexico (in red; Gallagher and Sheldon, 2016), and 19NOD04 in Myanmar (in black; this study). Soil wetness unit (dimensionless) varies between 0 and 1, indicating relative saturation between completely dry conditions and completely saturated conditions, respectively; satellite data span over the 2015-2020 period and were averaged daily (curve: average; shaded area: standard deviation).

A winter bias in carbonate growth contrasts the summer bias found in Tibetan carbonates, also grown under a well-established monsoonal regime (Quade et al., 2013; Burgener et al., 2018). The soil annual hydrological budget and temperature variation in Myanmar are significantly different from those of Tibet, providing potential explanations for this discrepancy. Monsoonal rainfall in Tibet is less intense (MAP commonly < 500 mm) and the rainy season is shorter. Soil wetness peaks in late summer (late August) and soils quickly dry (Fig. 6), potentially allowing carbonate to grow in early Fall. Unlike in Myanmar, where winter temperatures remain mild (CMMT > 15°C), Tibetan winter temperatures drop below freezing, drastically inhibiting evaporation and evapotranspiration and decreasing calcium activity. Soil water freezing favors cryogenic carbonate formation, which is associated with disequilibrium effects in clumped isotopic

composition and commonly drives $T\Delta_{47}$ values up; the contribution of this process in Tibetan carbonates remains debated (Burgener et al., 2018). A renewal of pedogenic carbonate growth in late spring and early summer, as proposed by Quade et al. (2013), is additionally possible when soils defrost before the rainy season.

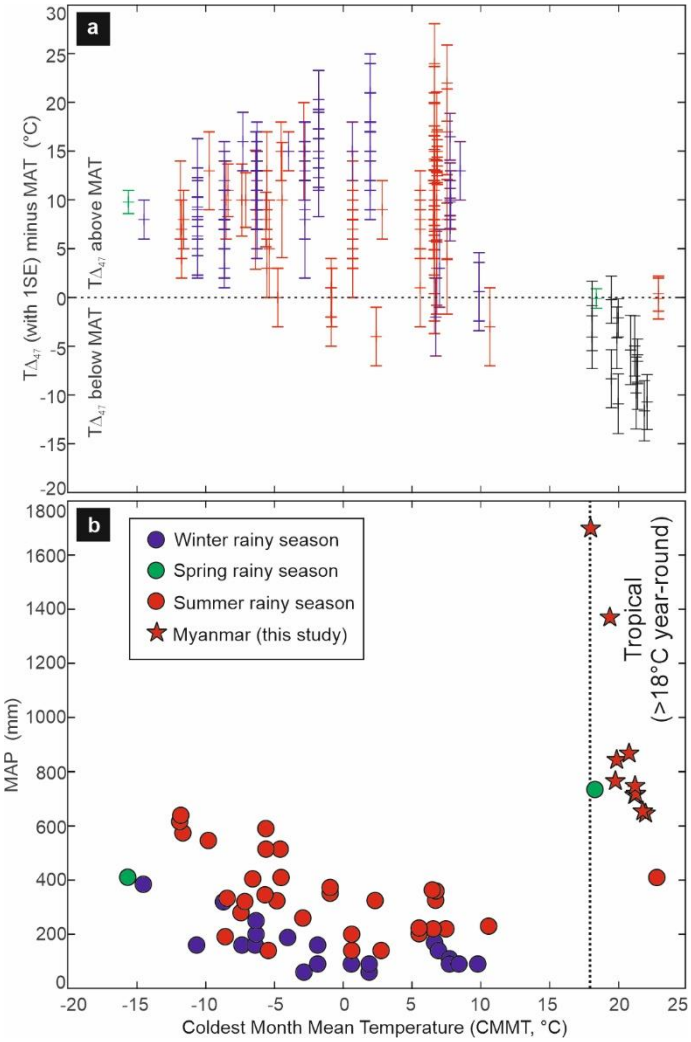

Figure 7. (a) $T\Delta_{47}$ values minus MAT of the same sites compared to their Coldest Month Mean Temperature (CMMT); $T\Delta_{47}$ error bars correspond to 1 SE. $T\Delta_{47}$ values from previous sites are from Kelson et al. (2020); CMMT, MAT, and MAP of Burmese sites from Worldclim 2.1; CMMT, MAT, and MAP from other sites from Kelson et al. (2020) or Worldclim 2.1 if not provided. **(b)** CMMT and MAP at the study sites (black crosses) compared to previously published soil carbonate clumped isotope data (from Kelson et al., 2020). Previously published sites are sorted according to their prominent rainy season on both panels: winter (blue crosses), spring (green crosses) and summer (red crosses); color coding is the same for both panels.

The apparent winter bias recorded in the Burmese pedogenic carbonates is so far unique in the clumped isotopic record of Quaternary carbonates (Fig. 7a). This is likely because the Burmese samples presented here represent an environment that is not previously addressed in clumped isotope studies, as this environment is both wetter and warmer (as demonstrated by a high CMMT; Fig 7b). Most clumped isotope data screened for robustness by Kelson et al. (2020) --more than 2 replicates, sampling depth ≥40 cm-- come from localities with MAP < 500 mm and more evenly distributed rainfall than the monsoonal domain, resulting in low levels of soil wetness year-round, even during the (weak) rainy season(s) (such as seen in the American Southwest; Fig. 6). All previous clumped isotope data sites also display cold CMMT (< 10 °C), which likely inhibits pedogenic carbonate growth during the cold season. Of the previously studied soil carbonate localities, only those in Ethiopia and Kenya fall within the tropical climate domain and experience high CMMT (18-23 °C) similar to our Burmese sites (Passey et al., 2010). The Kenyan site experiences evenly distributed, moderate rainfall over the year, peaking in spring (MAP: 736 mm), while the Ethiopian localities are much drier (MAP: 410 mm) and go through two dry seasons, in winter and late spring-early summer. Both rainfall distributions likely favor multiple yearly episodes of carbonate growth.

The $T\Delta_{47}$ values at both sites are in agreement with MAT (Fig. 7b), but these sites have a narrow seasonal range of temperature variation (< ±4 °C), and it is difficult to detect seasonal bias from $T\Delta_{47}$ alone.

5.3 Local parameters influencing carbonate growth and isotopic signature within the tropical domain

The variation in oxygen and carbon isotopic data among our sites suggests that multiple local factors influence carbonate growth and its isotopic signature within the Burmese lowlands.

We hypothesize that the variation in $\delta^{18}O$ values reflects the seasonal variation in parent waters and slight differences in timing of carbonate formation. One countering hypothesis is that evaporation could explain the higher $\delta^{18}O$ values observed. Evaporation in soils commonly drives carbonate $\delta^{18}O$ values up and is more likely to occur under arid conditions (Cerling and Quade, 1993; Beverly et al., 2020). However, in our dataset, the lowest carbonate $\delta^{18}O$ values are only present at the drier sites of study. Thus we think that spatial changes in evaporation effects have likely little impact on the spread of $\delta^{18}O$ values in our dataset. Another potential explanation is that that variation in $\delta^{18}O$ values could be due to age differences in the pedogenic carbonates. Interestingly, the coldest $T\Delta_{47}$ values in our Quaternary record are associated with the lowest water $\delta^{18}O$ values (-9 to -6 ‰ VSMOW; Fig. 4b), similar to rainfall $\delta^{18}O$ values reached at the end of the monsoon season (Fig. 3b), while the warmest temperatures are associated with higher $\delta^{18}O$ values (-6 to -1 ‰ VSMOW), typical of spring rainfall. These variations cannot be explained by differences in the ages of the pedogenic carbonates; carbonates grown during glacials --thus displaying the coldest temperatures-- would have higher water $\delta^{18}O$ values than carbonate grown during interglacials, as documented in Burmese speleothems (Liu et al., 2020). Instead, differences in seasonal timing of carbonate formation and parent water $\delta^{18}O$ best explain the observed variation in carbonate $\delta^{18}O$ values. The entire range of modern seasonal rainfall $\delta^{18}O$ values is covered in the range of calculated soil water $\delta^{18}O$ values, suggesting the variation is due to differences in the seasonal timing of carbonate growth. Recent studies have shown that carbonates often incorporate the $\delta^{18}O$ values of water that is contemporaneous with or directly preceding the period of carbonate growth rather than carry over soil water $\delta^{18}O$ values from out-of-season (Gallagher and Sheldon, 2016; Fischer-Femal and Bowen, 2021). Accordingly, the coldest $T\Delta_{47}$ values and lowest $\delta^{18}O$ values are compatible with carbonate growth in early winter with minimum soil water storage (1-3 months), incorporating late monsoonal waters; in contrast, warmer $T\Delta_{47}$ values and higher $\delta^{18}O$ values are compatible with growth in early spring, enriched in ^{18}O due to incorporation of spring rainwater or evaporation (Fig 4b).

Based solely on soil water $\delta^{18}O$ values, our limited dataset suggests that carbonate at drier sites (MAP <800 mm) grows preferentially in winter while growth at wetter sites (MAP >800 mm) is delayed towards early spring (Fig. 4b). The uncertainty around $T\Delta_{47}$ values remains too large to confirm that the same MAP-dependency is seen in growth temperatures. Individual carbonate nodules yield water $\delta^{18}O$ values compatible with winter and spring rain composition at the same locality, together with a wide range of $T\Delta_{47}$ values (15 ± 6 and 23 ± 4 °C 2 SE at site 19NOD06; Table 1), suggesting that MAP is not the only relevant factor impacting carbonate growth temperatures. Local (meter-scale) differences in landscape position, soil texture, or plant water use could impact soil water storage and explain some of the observed isotopic variability (Kelson et al., 2020).

The range of carbonate $\delta^{13}C$ values is particularly wide: there is an 11 ‰ difference between the most ^{13}C-depleted samples in the wet domain and the least ^{13}C-depleted samples in the dry domain. This difference cannot be explained by a varying amount of C4 plants, as organic matter $\delta^{13}C$ values do not show any marked contribution from C4 plants even at the driest sites (e.g. $\delta^{13}C$ always < -20 ‰ VPDB). Decreased water stress on Burmese C3 plants during glacials could potentially account for 3-5 ‰ of depletion in the pedogenic carbonates of the wetter sites (Kohn, 2010), but fails to explain the much wider range of $\delta^{13}C$ values. Seasonal variations in soil respiration rate and/or isotopic composition significantly impact soil CO_2 $\delta^{13}C$ values (Breecker et al., 2009) and could potentially explain part of this difference, as already proposed for other past monsoonal C3 records (Licht et al., 2020). Low rates and high $\delta^{13}C$ values of winter soil respiration followed by higher rates and lower $\delta^{13}C$ values of early spring respiration could partly explain the observed difference between sites on both ends of the $\delta^{13}C$ spectrum.

Stable isotopic data thus suggest that carbonate growth timing in Myanmar varies from early winter to early spring and that this variation is partly controlled by the local rainfall amount, unlike what is found at sites at higher latitudes. More generally, carbonate $\delta^{13}C$ and $\delta^{18}O$ values are not positively correlated as would be expected of temperate and arid region soils, where the effects of soil evaporation and respiration are the main drivers in changing those values (Fischer-Femal and Bowen, 2021; Broz et al., 2021). We hypothesize that overall higher soil wetness year-round in central Myanmar minimizes this covariation in comparison to temperate carbonate-rich soils, while making the bulk isotopic composition and $T\Delta_{47}$ values particularly sensitive to the seasonal rainfall distribution. Other eco-hydrological factors are likely also at play but remain to be identified with a more thorough sampling and systematic study of soil features. The soil texture, Bk horizon depth and dominant vegetation at each locality are described in Supplementary Table 1 and do not covary with bulk and clumped isotope composition (not shown). Importantly, Bk depth appears independent of local MAP, unlike observed in the temperate domain (Retallack, 2005). Our results thus highlight that carbonates grown under tropical conditions follow different growth patterns and isotope systematics than their temperate counterparts.

5.4 Implications for paleoenvironmental studies

Our dataset illustrates the high bulk and clumped isotope variability found in a limited geographical area in the tropical climate domain (ca. 10 ‰ for C and O isotopic data and 10 °C for $T\Delta_{47}$ values), driven by small changes in carbonate growth season influenced by local hydrological processes. This variability alone could explain a significant part of the variations found in several past bulk and clumped isotopic records without requiring dramatic changes of climate or elevation (Page et al., 2019). The processes and seasonal biases impacting carbonate growth in Myanmar today are also expected to be common in paleosols during Greenhouse intervals, which are associated with higher CMMT at mid-latitude, a wide spread of tropical ecosystems (Wing and Greenwood 1993; Toumoulin et al., 2021), and a more active hydrological cycle resulting in locally increased rainfall seasonality, as is seen in Paleogene Myanmar (Licht et al., 2014b). In particular, our results open the way for a reinterpretation of past bulk and clumped isotopic data used for the paleoaltimetry of Tibetan carbonates, which have so far systematically been interpreted as growing in

summer or equally throughout the year (e.g. Botsyun et al., 2019); low $\delta^{18}O$ values (<-10 ‰ VPDB) and cold $T\Delta_{47}$ values (<25 °C) are, in this framework, considered as reflecting high elevation. While some Paleogene sites display reconstructed water $\delta^{18}O$ values that are too low (<-14 ‰ VPDB) to be solely created by a monsoonal isotopic signature and thus require high elevations to explain them (Ingalls et al., 2018; Fang et al., 2020), others display bulk and clumped isotopic values similar to what we find today in Myanmar, and can alternatively reflect a monsoonal signature in carbonate growth at low elevation (Xiong et al., 2020). Moreover, decreasing rainfall amount and winter temperatures during gradual Tibetan uplift in the monsoonal domain should gradually move the carbonate growth season from early spring to winter, late fall, and eventually early fall and/or late spring, once the winters are too cold to favor carbonate growth and the rainy season is limited to a few months in the summer. This complex evolution makes paleoaltimetry estimates based on soil carbonate data more challenging in the monsoonal domain and for past tropical climates.

5.5 An isotopic signature for past rainfall distribution?

While making paleoelevation estimates based solely on pedogenic carbonate bulk and clumped isotope data appears challenging, these data can provide unique insight into rainfall dynamics when MAT or elevation are independently constrained. In particular, the climatic patterns proposed as the origin of the Burmese winter bias in $T\Delta_{47}$ values, i.e. wet summers combined with dry and warm winter season, are diagnostic of tropical seasonal climates with a winter dry season (climate classes Am and Aw sensu Köppen), today typical of monsoonal areas at low altitude. Lower $T\Delta_{47}$ values than MAT should thus provide a proxy for tropical seasonal climates and possible test for the monsoonal nature of rainfall in tropical paleosols when combined with other proxy data. In addition, our observations suggest that C and O isotopic data could potentially provide insights into rainfall amount, though their MAP-dependency remains to be confirmed with a more systematic study of Quaternary tropical pedogenic carbonates and soil waters.

In this light, the results from the Miocene Natma Formation are meaningful and provide a proof-of-concept example for the usefulness of combined bulk and clumped isotope analysis in the tropical domain when the climate is independently constrained. Natma pedogenic carbonates yield low $T\Delta_{47}$ values (20-23 °C), high $\delta^{18}O$ (>-4 ‰ VPDB) and low $\delta^{13}C$ (< -10 ‰ VPDB) values. Following regular isotopic interpretative keys used in the temperate domain, $T\Delta_{47}$ values could be interpreted as reflecting colder summers than today's (Kelson et al., 2020), and high $\delta^{18}O$ values would reflect less monsoonal rainfall while low $\delta^{13}C$ would mean overall wetter conditions (Caves et al., 2015). These interpretations suggest a colder and wetter climate at the time of the Natma Formation, with limited monsoons and more evenly distributed rainfall over the year. They contrast with independent lines of evidence for a warmer late early to early middle Miocene globally (Steinthorsdottir et al., 2020) with intense Asian monsoons (Clift et al., 2008), and raise preservation issues, as higher but less seasonal rainfall would likely favor the dissolution of pedogenic carbonate. In contrast, fossil wood specimens of the Natma Formation reflect different ecotones of seasonal forests with coastal, mixed to dry deciduous, and wet evergreen species, suggesting a warm, seasonal monsoonal climate during the late early Miocene at least as wet as today, and possibly wetter summers (Gentis et al., 2019). In this

context, low $T\Delta_{47}$ values relative to the local MAT (<25 °C) in Natma pedogenic carbonates corroborate a summer rainy season (Fig. 4b), while high $\delta^{18}O$ (>-4 ‰ VPDB) values and low $\delta^{13}C$ (< -10 ‰ VPDB) values fall on the "wet" side of the carbonate spectrum, similar to what is found today in our field area (Fig. 4a), suggesting a carbonate growth season in early spring. This interpretation is more in line with the fossil wood assemblage, and suggests modern-like monsoonal rainfall in Myanmar in the late early Miocene. This example illustrates how different isotopic systematics are between pedogenic carbonates in the temperate and tropical domains, and how applying interpretative keys based on mid-latitude carbonate behavior can significantly impact paleoclimatic interpretations in the tropical domain. This complexity is particularly expected for $T\Delta_{47}$ values of pedogenic carbonates from past greenhouse climates, when winter temperatures were globally higher.

6. Conclusion

Relatively low $T\Delta_{47}$ values (<25 °C) in Quaternary soil carbonates from central Myanmar indicate a bias in carbonate growth timing toward winter and early spring. We attribute the cold season bias to the combined effects of warm winter temperatures and intense rainfall during the summer and fall, conditions that are typical of tropical climates with monsoonal rainfall. These conditions allow for carbonate growth in areas where MAP today exceeds 1700 mm. Oxygen and carbon isotopic data suggest that carbonate growth timing locally varies from early winter to early spring, with decreasing incorporation of ^{18}O-depleted monsoonal waters throughout the growth span. This trend is partly influenced by local MAP, with the wettest sites possibly delayed to early spring. Our results confirm that rainfall annual distribution and amount significantly impact the season of carbonate growth and its bulk and clumped isotopic record (Peters et al., 2013; Gallagher and Sheldon, 2016; Burgener et al., 2016; Kelson et al., 2020). We suggest that this expression is particularly important in tropical areas, where high soil wetness year-round narrows carbonate growth to the driest months and makes it particularly sensitive to the seasonal distribution of rainfall. This sensitivity is also enhanced by high CMMT, allowing carbonate growth to move outside the warmest months of the year. This high sensitivity is expected to be more prominent in the geological record during times with higher temperatures and greater expansion of the tropical realm. "Cold" $T\Delta_{47}$ records in Asian paleosols, often interpreted through the lens of evolving topography, might instead provide a possible signature for tropical seasonal climate and monsoonal rainfall. Our understanding of pedogenic carbonate growth dynamics has been so far strongly biased toward temperate ecosystems; our results show that pedogenic carbonates grown under Burmese tropical conditions follow different dynamics and isotope systematics. These remain to be further documented and expanded to other tropical soil carbonates to gain a more complete understanding of their growth under different conditions and the resulting implications for paleoenvironmental reconstructions.

Acknowledgments

This study was financially supported by the University of Washington and European Research Council

consolidator grant MAGIC 649081. We thank L. Burgener, J. Harlé, S. Shekut, C. Bourgeois, Kyi Kyi Thein, Hnin Hnin Swe, Myat Kay Thi, A. Gough, D. Perez-Pinedo, J. Westerweel, and P. Roperch for prolific discussions and assistance in the field and lab. Datasets for this research are included in the supplementary information files and archived on EarthChem (https://doi.org/10.26022/IEDA/112320).

References

Anderson, N. T., Kelson, J. R., Kele, S., Daëron, M., Bonifacie, M., Horita, J., ... & Bergmann, K. D. (2021). A unified clumped isotope thermometer calibration (0.5–1100° C) using carbonate- based standardization. *Geophysical Research Letters*, e2020GL092069.

Araguás- Araguás, L., Froehlich, K., & Rozanski, K. (1998). Stable isotope composition of precipitation over southeast Asia. *Journal of Geophysical Research: Atmospheres*, *103*(D22), 28721-28742.

Belousov, A., Belousova, M., Zaw, K., Streck, M. J., Bindeman, I., Meffre, S., & Vasconcelos, P. (2018). Holocene eruptions of Mt. Popa, Myanmar: Volcanological evidence of the ongoing subduction of Indian Plate along Arakan Trench. *Journal of Volcanology and Geothermal Research*, *360*, 126-138.

Broz, A., Retallack, G. J., Maxwell, T. M., & Silva, L. C. (2021). A record of vapour pressure deficit preserved in wood and soil across biomes. *Scientific reports*, *11*(1), 1-12.

Bernasconi, S., Daëron, M., Bergmann, K., Bonifacie, M., Meckler, A. N., Affek, H., ... & Ziegler, M. (2021). InterCarb: A community effort to improve inter-laboratory standardization of the carbonate clumped isotope thermometer using carbonate standards.

Bettis III, E. A., Milius, A. K., Carpenter, S. J., Larick, R., Zaim, Y., Rizal, Y., ... & Bronto, S. (2009). Way out of Africa: Early Pleistocene paleoenvironments inhabited by Homo erectus in Sangiran, Java. *Journal of Human Evolution*, *56*(1), 11-24.

Beverly, E., Levin, N. E., Passey, B. H., Aron, P. G., Yarian, D. A., Page, M., & Pelletier, E. M. (2020). Triple oxygen and clumped isotopes in modern soil carbonate along an aridity gradient in the Serengeti, Tanzania. *Earth and Space Science Open Archive ESSOAr*.

Botsyun, S., Sepulchre, P., Donnadieu, Y., Risi, C., Licht, A., & Rugenstein, J. K. C. (2019). Revised paleoaltimetry data show low Tibetan Plateau elevation during the Eocene. *Science*, *363*(6430).

Breecker, D. O., Sharp, Z. D., & McFadden, L. D. (2009). Seasonal bias in the formation and stable isotopic composition of pedogenic carbonate in modern soils from central New Mexico, USA. *Geological Society of America Bulletin*, *121*(3-4), 630-640.

Breecker, D. O., Sharp, Z. D., & McFadden, L. D. (2010). Atmospheric CO2 concentrations during ancient greenhouse climates were similar to those predicted for AD 2100. *Proceedings of the National Academy of*

Sciences, *107*(2), 576-580.

Burgener, L., Huntington, K. W., Hoke, G. D., Schauer, A., Ringham, M. C., Latorre, C., & Díaz, F. P. (2016). Variations in soil carbonate formation and seasonal bias over> 4 km of relief in the western Andes (30 S) revealed by clumped isotope thermometry. *Earth and Planetary Science Letters*, *441*, 188-199.

Burgener, L. K., Huntington, K. W., Sletten, R., Watkins, J. M., Quade, J., & Hallet, B. (2018). Clumped isotope constraints on equilibrium carbonate formation and kinetic isotope effects in freezing soils. *Geochimica et Cosmochimica Acta*, *235*, 402-430.

Caves, J. K., Winnick, M. J., Graham, S. A., Sjostrom, D. J., Mulch, A., & Chamberlain, C. P. (2015). Role of the westerlies in Central Asia climate over the Cenozoic. *Earth and Planetary Science Letters*, *428*, 33-43.

Cerling, T. E., Solomon, D. K., Quade, J. A. Y., & Bowman, J. R. (1991). On the isotopic composition of carbon in soil carbon dioxide. *Geochimica et Cosmochimica Acta*, *55*(11), 3403-3405.

Clift, P. D., Hodges, K. V., Heslop, D., Hannigan, R., Van Long, H., & Calves, G. (2008). Correlation of Himalayan exhumation rates and Asian monsoon intensity. *Nature geoscience*, *1*(12), 875-880.

Colin, C., Bertaux, J., Turpin, L., & Kissel, C. (2001). Dynamique de l'érosion dans le bassin versant de l'Irrawaddy au cours des deux derniers cycles climatiques (280–0 ka). *Comptes Rendus de l'Académie des Sciences-Series IIA-Earth and Planetary Science*, *332*(8), 483-489.

Cerling, T. E., & Quade, J. (1993). Stable carbon and oxygen isotopes in soil carbonates. *Climate change in continental isotopic records. Geophysical Monograph*, *78*, 217-231.

DiNezio, P. N., Tierney, J. E., Otto-Bliesner, B. L., Timmermann, A., Bhattacharya, T., Rosenbloom, N., & Brady, E. (2018). Glacial changes in tropical climate amplified by the Indian Ocean. *Science advances*, *4*(12), eaat9658.

Ehleringer, J. R., Lin, Z. F., Field, C. B., Sun, G. C., & Kuo, C. Y. (1987). Leaf carbon isotope ratios of plants from a subtropical monsoon forest. *Oecologia*, *72*(1), 109-114.

Fang, X., Dupont-Nivet, G., Wang, C., Song, C., Meng, Q., Zhang, W., ... & Chen, Y. (2020). Revised chronology of central Tibet uplift (Lunpola Basin). *Science Advances*, *6*(50), eaba7298.

Fick, S. E., & Hijmans, R. J. (2017). WorldClim 2: new 1- km spatial resolution climate surfaces for global land areas. *International journal of climatology*, *37*(12), 4302-4315.

Fischer-Femal, B. J., & Bowen, G. J. (2021). Coupled carbon and oxygen isotope model for pedogenic carbonates. *Geochimica et Cosmochimica Acta*, *294*, 126-144.

Gallagher, T. M., & Sheldon, N. D. (2016). Combining soil water balance and clumped isotopes to

understand the nature and timing of pedogenic carbonate formation. *Chemical Geology*, *435*, 79-91.

Gallagher, T. M., Hren, M., & Sheldon, N. D. (2019). The effect of soil temperature seasonality on climate reconstructions from paleosols. *American Journal of Science*, *319*(7), 549-581.

Gentis, N., Boura, A., & De Franceschi, D. (2019). Fossil wood from the Miocene of Myanmar: application to the reconstruction of monsoonal paleoenvironments. *Congrès Agora paleobotanica*, Jul 2019, Lille, France. [note: a scientific paper based on this conference talk is in review at *Geodiversitas* and available on ESSOAR: https://www.essoar.org/doi/abs/10.1002/essoar.10506983.1].

Hanpattanakit, P., Leclerc, M. Y., Mcmillan, A. M., Limtong, P., Maeght, J. L., Panuthai, S., ... & Chidthaisong, A. (2015). Multiple timescale variations and controls of soil respiration in a tropical dry dipterocarp forest, western Thailand. *Plant and soil*, *390*(1), 167-181.

Hoke, G. D., Liu-Zeng, J., Hren, M. T., Wissink, G. K., & Garzione, C. N. (2014). Stable isotopes reveal high southeast Tibetan Plateau margin since the Paleogene. *Earth and Planetary Science Letters*, *394*, 270-278.

Huth, T. E., Cerling, T. E., Marchetti, D. W., Bowling, D. R., Ellwein, A. L., & Passey, B. H. (2019). Seasonal bias in soil carbonate formation and its implications for interpreting high- resolution paleoarchives: Evidence from southern Utah. *Journal of Geophysical Research: Biogeosciences*, *124*(3), 616-632.

Ingalls, M., Rowley, D., Olack, G., Currie, B., Li, S., Schmidt, J., ... & Colman, A. (2018). Paleocene to Pliocene low-latitude, high-elevation basins of southern Tibet: Implications for tectonic models of India-Asia collision, Cenozoic climate, and geochemical weathering. *GSA Bulletin*, *130*(1-2), 307-330.

Kelson, J. R., Huntington, K. W., Schauer, A. J., Saenger, C., & Lechler, A. R. (2017). Toward a universal carbonate clumped isotope calibration: Diverse synthesis and preparatory methods suggest a single temperature relationship. *Geochimica et Cosmochimica Acta*, *197*, 104-131.

Kelson, J. R., Huntington, K. W., Breecker, D. O., Burgener, L. K., Gallagher, T. M., Hoke, G. D., & Petersen, S. V. (2020). A proxy for all seasons? A synthesis of clumped isotope data from Holocene soil carbonates. *Quaternary Science Reviews*, *234*, 106259.

Khaing, T. T., Pasion, B. O., Lapuz, R. S., & Tomlinson, K. W. (2019). Determinants of composition, diversity and structure in a seasonally dry forest in Myanmar. *Global Ecology and Conservation*, *19*, e00669.

Kim, S. T., & O'Neil, J. R. (1997). Equilibrium and nonequilibrium oxygen isotope effects in synthetic carbonates. *Geochimica et cosmochimica acta*, *61*(16), 3461-3475.

Kohn, M. J. (2010). Carbon isotope compositions of terrestrial C3 plants as indicators of (paleo) ecology and (paleo) climate. *Proceedings of the National Academy of Sciences*, *107*(46), 19691-19695.

Kume, T., Tanaka, N., Yoshifuji, N., Chatchai, T., Igarashi, Y., Suzuki, M., & Hashimoto, S. (2013). Soil respiration in response to year- to- year variations in rainfall in a tropical seasonal forest in northern Thailand. *Ecohydrology*, *6*(1), 134-141.

Lai Lai Aung, Ei EI Zin, Pwint Theingi, Naw Elvera, Phyu Phyu Aung, Thu Thu Han, Yamon Oo, & Skaland R.G. (2017). Myanmar Climate Report, *MET Report* No. 9/2017.

Licht, A., Van Cappelle, M., Abels, H. A., Ladant, J. B., Trabucho-Alexandre, J., France-Lanord, C., ... & Terry Jr, D. (2014b). Asian monsoons in a late Eocene greenhouse world. *Nature* 513, 501-506.

Licht, A., Dupont-Nivet, G., Meijer, N., Rugenstein, J. C., Schauer, A., Fiebig, J., ... & Guo, Z. (2020). Decline of soil respiration in northeastern Tibet through the transition into the Oligocene icehouse. *Palaeogeography, Palaeoclimatology, Palaeoecology*, *560*, 110016.

Liu, G., Li, X., Chiang, H. W., Cheng, H., Yuan, S., Chawchai, S., ... & Wang, X. (2020). On the glacial-interglacial variability of the Asian monsoon in speleothem δ18O records. *Science advances*, *6*(7), eaay8189.

Meena, A., Hanief, M., Dinakaran, J., & Rao, K. S. (2020). Soil moisture controls the spatio-temporal pattern of soil respiration under different land use systems in a semi-arid ecosystem of Delhi, India. *Ecological Processes*, *9*(1), 1-13.

Montanez, I. P. (2013). Modern soil system constraints on reconstructing deep-time atmospheric CO2. *Geochimica et Cosmochimica Acta*, *101*, 57-75.

Menne, M. J., Williams, C. N., Gleason, B. E., Rennie, J. J., & Lawrimore, J. H. (2018). The global historical climatology network monthly temperature dataset, version 4. *Journal of Climate*, *31*(24), 9835-9854.

Page, M., Licht, A., Dupont-Nivet, G., Meijer, N., Barbolini, N., Hoorn, C., ... & Guo, Z. (2019). Synchronous cooling and decline in monsoonal rainfall in northeastern Tibet during the fall into the Oligocene icehouse. *Geology*, *47*(3), 203-206.

Peters, N. A., Huntington, K. W., & Hoke, G. D. (2013). Hot or not? Impact of seasonally variable soil carbonate formation on paleotemperature and O-isotope records from clumped isotope thermometry. *Earth and Planetary Science Letters*, *361*, 208-218.

Pivnik, D. A., Nahm, J., Tucker, R. S., Smith, G. O., Nyein, K., Nyunt, M., & Maung, P. H. (1998). Polyphase deformation in a fore-arc/back-arc basin, Salin subbasin, Myanmar (Burma). *AAPG bulletin*, *82*(10), 1837-1856.

Passey, B. H., Levin, N. E., Cerling, T. E., Brown, F. H., & Eiler, J. M. (2010). High-temperature environments of human evolution in East Africa based on bond ordering in paleosol carbonates. *Proceedings*

of the National Academy of Sciences, *107*(25), 11245-11249.

Quade, J., Breecker, D. O., Daëron, M., & Eiler, J. (2011). The paleoaltimetry of Tibet: An isotopic perspective. *American Journal of Science*, *311*(2), 77-115.

Quade, J., Eiler, J., Daeron, M., & Achyuthan, H. (2013). The clumped isotope geothermometer in soil and paleosol carbonate. *Geochimica et Cosmochimica Acta*, *105*, 92-107.

Railsback, L. B. (2021). Pedogenic carbonate nodules from a forested region of humid climate in central Tennessee, USA, and their implications for interpretation of C3-C4 relationships and seasonality of meteoric precipitation from carbon isotope (δ13C) data. *CATENA*, *200*, 105169.

Reichle, R., G. De Lannoy, R. D. Koster, W. T. Crow, J. S. Kimball, and Q. Liu. 2018. SMAP L4 Global 3-hourly 9 km EASE-Grid Surface and Root Zone Soil Moisture Analysis Update, Version 4. Boulder, Colorado USA. *NASA National Snow and Ice Data Center Distributed Active Archive Center*. https://doi.org/10.5067/60HB8VIP2T8W. [Date Accessed].

Retallack, G. J. (2005). Pedogenic carbonate proxies for amount and seasonality of precipitation in paleosols. *Geology*, *33*(4), 333-336.

Romanek, C. S., Grossman, E. L., & Morse, J. W. (1992). Carbon isotopic fractionation in synthetic aragonite and calcite: effects of temperature and precipitation rate. *Geochimica et cosmochimica acta*, *56*(1), 419-430.

Rubio, V. E., & Detto, M. (2017). Spatiotemporal variability of soil respiration in a seasonal tropical forest. *Ecology and evolution*, *7*(17), 7104-7116.

Saraswat, R., Lea, D. W., Nigam, R., Mackensen, A., & Naik, D. K. (2013). Deglaciation in the tropical Indian Ocean driven by interplay between the regional monsoon and global teleconnections. *Earth and Planetary Science Letters*, *375*, 166-175.

Singh, L., & Singh, S. (1972). Chemical and morphological composition of kankar nodules in soils of the Vindahyan region of Mirzapur, India. *Geoderma*, *7*(3-4), 269-276.

Stamp, L. D. (1940). The Irrawaddy River. *The Geographical Journal*, *95*(5), 329-352.

Steinthorsdottir, M., Coxall, H. K., de Boer, A. M., Huber, M., Barbolini, N., Bradshaw, C. D., ... & Strömberg, C. A. E. (2020). The Miocene: the Future of the Past. *Paleoceanography and Paleoclimatology*, e2020PA004037.

Toumoulin, A., Tardif, D., Donnadieu, Y., Licht, A., Ladant, J. B., Kunzmann, L., & Dupont-Nivet, G. (2021). Evolution of continental temperature seasonality from the Eocene greenhouse to the Oligocene icehouse-A model-data comparison. *Climate of the Past Discussions*, 1-30. (https://doi.org/10.5194/cp-2021-

Van Der Kaars, S., & Dam, R. (1997). Vegetation and climate change in West-Java, Indonesia during the last 135,000 years. *Quaternary International*, *37*, 67-71.

Westerweel, J., Licht, A., Cogné, N., Roperch, P., Dupont- Nivet, G., Kay Thi, M., ... & Wa Aung, D. (2020). Burma Terrane collision and northward indentation in the Eastern Himalayas recorded in the Eocene- Miocene Chindwin Basin (Myanmar). *Tectonics*, *39*(10), e2020TC006413.

Wing, S. L., & Greenwood, D. R. (1993). Fossils and fossil climate: the case for equable continental interiors in the Eocene. *Philosophical transactions of the royal society of London. Series B: Biological Sciences*, *341*(1297), 243-252.

Xiong, Z., Ding, L., Spicer, R. A., Farnsworth, A., Wang, X., Valdes, P. J., ... & Yue, Y. (2020). The early Eocene rise of the Gonjo Basin, SE Tibet: From low desert to high forest. *Earth and Planetary Science Letters*, *543*, 116312.

Supplementary table 2C: Clumped Isotope Data Summary

UM d13C and d18O std error from sample replicates < 0.01 | UM D47 std error from sample replicates < 0.01 | UM D47 stdev from long-term carbonate standards = *0.0145*

UW d13C and d18O std error from sample replicates < 0.01 | UW D47 std error from sample replicates < 0.01 | UW D47 stdev from long-term carbonate standards = *0.0261*

Sample name	Analysis Location	Replicate ID	d13C vs VPDB (formal) (permil)	d13C stderr	d18O vs VPDB (formal) (permil)	d18O stderr	d18O vs VSMOW	α	δ18O soil water (VSMOW)	D47 Intercarb acid (permil)	D47 stderr (from sample replicates)	D47 sterr (from longer-term standards)	T(D47) (°C)	*T error (replicates)*	*T error (standards)*	T error (°C)
17NOD01	UW Isolab	200319_3_M1-1	-6.11		-4.84					0.7043						
		191122_2_M1-1	-6.08		-4.86					0.6601						
		200215_3_M1-1	-6.08		-4.73					0.7252						
		180406_3_M1-1`	-6.12		-5.03					0.7007						
		180410_4_M1-2'	-5.98		-3.91					0.6956						
		180412_1_M1-3`	-6.12		-3.90					0.6472						
		180412_2_M1-4`	-6.09		-4.32					0.6991						
		191115_3_M1-1	-6.07		-4.85					0.6910						
17NOD01			-6.08	0.02	-4.56	0.16	26.21	1.03	-2.91	0.6904	0.0089	0.0092	21.4	2.9	3.0	3.0
17NOD04	UW Isolab	191121_2_M4	-6.78		-10.05					0.6330						
		200215_2_M4-3	-6.81		-9.98					0.7237						
		200311_5_M4	-6.94		-10.12					0.6451						
		200313_6_M4	-6.96		-10.12					0.6792						
		200319_5_M4	-7.05		-10.16					0.7089						
		200702_3_M4	-6.94		-10.14					0.7310						
		200826_5_M4	-6.99		-10.19					0.7220						
		200813_5_M4	-6.96		-10.07					0.7222						
		180514_4_M4-1	-6.96		-10.09					0.6984						
		180518_1_M4-1	-7.26		-10.07					0.6736						
		180518_2_M4-4	-7.03		-10.17					0.6999						
17NOD04			-6.97	0.04	-10.11	0.02	20.49	1.03	-8.73	0.6943	0.0099	0.0079	20.2	3.2	2.5	3.2
19NOD02	UW Isolab	200311_1_19NOD02	-10.15		-4.28					0.6761						
		200313_3_19NOD02	-10.18		-4.40					0.6873						
		200314_4_19NOD02	-10.13		-4.45					0.7026						
		200317_1_19NOD02	-10.21		-4.33					0.6843						
		200319_1_19NOD02	-10.23		-4.49					0.6736						
		200616_4_19NOD02	-10.16		-4.42					0.7150						
19NOD02			-10.18	0.02	-4.39	0.03	26.38	1.03	-2.70	0.6898	0.0065	0.0107	21.6	2.1	3.4	3.4
19NOD03	UW Isolab	200314_1_19NOD03	-10.20		-6.84					0.6581						
		200317_2_19NOD03	-10.24		-6.69					0.7283						
		200319_4_19NOD03	-10.24		-6.79					0.7213						
		200616_3_19NOD03	-10.11		-6.76					0.6931						
		200630_5_19NOD03	-10.04		-6.75					0.6731						
		200617_4_19NOD03	-10.14		-6.81					0.6956						
		200622_2_19NOD03	-10.11		-6.31					0.7061						
19NOD03			-10.16	0.03	-6.71	0.07	24.00	1.03	-5.47	0.6965	0.0095	0.0099	19.5	3.0	3.1	3.1
19NOD04_A	UW Isolab	191121_3_19NOD04	-14.73		-4.10					0.6821						
		191122_6_19NOD04	-14.72		-4.05					0.6658						
		200213_2_ND04_1	-14.73		-3.98					0.7395						
		200125_3_ND04_1	-14.68		-4.17					0.7376						
		200225_3_ND04_1	-14.76		-3.94					0.7122						
		200309_5_ND04_1	-14.67		-3.98					0.6683						

		200314_5_ND04_1	-14.69		-4.09					0.7354					
		200319_6_ND04_1	-14.79		-4.13					0.6973					
		200702_5_19ND04_1	-14.70		-4.21					0.7123					
19NOD04_A			-14.72	0.01	-4.07	0.03	26.71	1.03	-3.44	0.7056	0.0097	0.0087	16.6	3.0	2.7	3.0
19NOD04_B	UM	1886_19ND04-3-1	-13.94		-3.99					0.6669					
		1926_19ND04-3-2	-13.91		-3.95					0.6794					
		2058_19ND04-3	-13.93		-4.02					0.6808					
		2160_19ND04-3-1	-13.91		-4.05					0.6954					
19NOD04_B			-13.92	0.01	-4.00	0.02	26.79	1.03	-1.68	0.6806	0.0058	0.0073	24.7	2.0	2.4	2.4
19NOD06_A	UW Isolab	191121_6_19NOD06	-8.45		-7.39					0.6865					
		200125_5_ND06_1	-8.40		-7.47					0.7299					
		200225_5_ND06_1	-8.53		-7.38					0.7130					
		200305_1_ND06_1	-8.41		-7.59					0.7458					
		200306_5_ND06_1	-8.42		-7.47					0.6834					
		200313_4_ND06_1	-8.43		-7.43					0.7200					
		200314_3_ND06_1	-8.44		-7.33					0.7190					
19NOD06_A			-8.44	0.02	-7.44	0.03	23.24	1.03	-7.36	0.7140	0.0085	0.0099	14.0	2.5	2.9	2.9
19NOD06_B	UM	1855_19NOD06-3-1	-8.32		-6.56					0.6911					
		1905_19NOD06-3-2	-8.32		-6.50					0.6743					
		2032_19NOD06-3-3	-8.39		-6.97					0.7009					
		2157_19NOD06-3-1	-8.34		-6.62					0.6861					
		2228_19NOD06-3-2	-8.31		-6.58					0.6838					
		2311_19NOD06-3-3	-8.31		-6.54					0.6810					
19NOD06_B			-8.33	0.01	-6.63	0.07	24.08	1.03	-4.69	0.6862	0.0037	0.0059	22.8	1.2	1.9	1.9
19NOD07	UW Isolab	191121_5_19NOD07	-6.95		-6.87					0.6614					
		191122_7_19NOD07	-6.95		-6.82					0.7372					
		200125_2_ND07_1	-6.90		-6.95					0.7398					
		200214_2_ND07_1	-6.97		-6.76					0.6997					
		200226_2_ND07_1	-7.00		-6.77					0.7308					
		200227_1_ND07_1	-7.01		-6.91					0.6582					
		200228_5_ND07_1	-7.01		-6.93					0.7034					
		200309_2_ND07_1	-6.93		-6.83					0.7241					
		200622_4_19ND07_1	-6.97		-6.97					0.7204					
		200311_3_ND07_1	-7.02		-6.73					0.6966					
19NOD07			-6.97	0.01	-6.85	0.03	23.84	1.03	-6.33	0.7072	0.0092	0.0083	16.1	2.8	2.5	2.8
19NOD08	UW Isolab	200124_3_ND08_1	-6.41		-8.99					0.6717					
		200220_1_ND08_1	-6.56		-8.91					0.7324					
		200229_5_ND08_1	-6.57		-9.00					0.7137					
		200303_1_ND08_1	-6.45		-8.99					0.7302					
		200304_3_ND08_1	-6.49		-9.10					0.6726					
		200305_6_ND08_1	-6.44		-9.02					0.7111					
		200702_2_19ND08_1	-6.51		-9.00					0.6684					
		200921_4_19ND08	-6.47		-8.71					0.7547					
		200907_2_19ND08	-6.45		-7.78					0.6499					
		200811_1_19ND08	-6.49		-9.10					0.7568					
19NOD08			-6.48	0.02	-8.86	0.13	21.78	1.03	-8.27	0.7061	0.0121	0.0083	16.4	3.7	2.5	3.7
19NOD09	UW Isolab	191122_1_19NOD09	-7.45		-7.48					0.6770					
		191122_5_19NOD09	-7.45		-7.55					0.6997					
		200125_4_ND09_2	-7.81		-7.35					0.6958					
		200214_3_ND09_2	-7.53		-6.99					0.7492					
		200213_5_ND09_2	-7.50		-7.47					0.7356					

		200225_4_ND09_2	-7.52		-7.38					0.7262					
		200619_4_19ND09_2	-7.77		-7.30					0.6940					
19NOD09			-7.57	0.06	-7.36	0.07	23.32	1.03	-7.10	0.7111	0.0099	0.0099	14.9	3.0	3.0	3.0
20NOD01	UW Isolab	200215_5_20NOD01_2	-7.21		-5.05					0.7401					
		200227_4_20NOD01_2	-7.92		-5.55					0.6714					
		200228_4_20NOD01_2	-7.76		-5.54					0.6956					
		200306_3_20NOD01_2	-7.82		-5.40					0.6756					
		200309_4_20NOD01_2	-7.75		-5.42					0.7027					
		200805_4_20NOD01	-7.67		-5.53					0.6682					
20NOD01			-7.69	0.10	-5.41	0.08	25.33	1.03	-3.89	0.6923	0.0111	0.0107	20.8	3.6	3.4	3.6
20NOD03_A	UW Isolab	200215_4_20NOD03_1	-9.91		-8.58					0.7275					
		200228_3_20NOD03_1	-9.96		-8.76					0.7237					
		200229_2_20NOD03_1	-9.95		-8.75					0.6769					
		200304_2_20NOD01_2	-7.80		-5.51					0.6785					
		200303_6_20NOD03_1	-9.93		-8.57					0.7511					
		200309_6_20NOD03_1	-9.78		-8.41					0.6800					
		200313_2_20NOD03_1	-9.82		-8.56					0.6875					
		200617_3_20NOD03_1	-9.90		-8.33					0.7092					
		200702_1_20NOD03	-9.84		-8.77					0.6943					
20NOD03_A			-9.66	0.23	-8.25	0.35	22.40	1.03	-7.46	0.7032	0.0087	0.0087	17.3	2.7	2.7	2.7
20NOD03_B	UM	1874_20ND03-3-1	-9.19		-7.12					0.6882					
		1919_20ND03-3-2	-9.19		-7.03					0.6913					
		2159_20ND03-3-1	-9.20		-7.13					0.7177					
		2232_20ND03-3-2	-9.17		-7.01					0.6888					
20NOD03_B			-9.19	0.01	-7.07	0.03	23.62	1.03	-5.84	0.6965	0.0071	0.0073	19.5	2.3	2.3	2.3
19NAT13	UW Isolab	200613_2_19NAT13	-10.37		-3.38					0.6768					
		200630_2_19NAT13	-10.15		-3.21					0.6998					
		200706_2_19NAT13	-10.14		-3.37					0.7651					
		200709_3_19NAT13	-10.09		-3.24					0.6705					
		200717_2_19NAT13	-10.20		-3.29					0.6842					
		200818_2_19NAT13	-10.19		-3.20					0.7130					
		200819_1_19NAT13	-6.32		-10.41					0.6559					
		200822_3_19NAT13	-10.10		-2.92					0.7155					
19NAT13			-9.70	0.48	-4.13	0.90	26.66	1.03	-2.96	0.6976	0.0121	0.0051	19.1	3.8	1.6	3.8
19NAT01	UW Isolab	200613_6_19NAT01	-9.93		-1.47					0.7098					
		200623_5_19NAT01	-10.11		-1.69					0.6853					
		200629_4_19NAT01	-9.86		-1.69					0.7054					
		200709_2_19NAT01	-9.81		-1.71					0.6598					
		200806_5_19NAT01	-9.83		-1.58					0.6804					
19NAT01			-9.91	0.06	-1.63	0.05	29.23	1.03	0.18	0.6881	0.0091	0.0065	22.2	2.9	2.1	2.9

Localities			Climate parameters from WorldClim V2, res: 5min				Clumped isotopic data										
age	location on fig. 1	name	MAT (in °C)	WMMT (in °C)	CMMT (in °C)	MAP (in mm)	*n*	Carbonate $\delta^{13}C$ (‰ VPDB)	$\delta^{13}C$ S.E. (‰)	Carbonate $\delta^{18}O$ (‰ VPDB)	$\delta^{18}O$ S.E. (‰)	$\Delta_{47\ I\text{-}CDES25}$ (‰)	Δ_{47} S.E. (‰)	$T\Delta_{47}$ (°C)	$T\Delta_{47}$ S.E. (°C)	Soil Water $\delta^{18}O$ (‰ VSMOW)	Soil Water $\delta^{18}O$ propagated S.E. (‰)
Quaternary soils	1	17NOD01	27.2	31.3	21.2	747	8	-6.08	0.02	-4.56	0.16	0.6904	0.0092	22.1	3.0	-2.8	0.6
	2	17NOD04	25.1	29.6	19.9	772	11	-6.97	0.04	-10.11	0.02	0.6943	0.0099	20.9	3.2	-8.6	0.7
	3	19NOD02	24.3	28.5	18.1	1701	6	-10.18	0.02	-4.39	0.03	0.6898	0.0107	22.3	3.5	-2.6	0.7
	3	19NOD03	24.3	28.5	18.1	1701	7	-10.16	0.03	-6.71	0.07	0.6965	0.0099	20.2	3.1	-5.3	0.6
	4	19NOD04	25.7	29.8	19.5	1372	9	-14.72	0.01	-4.07	0.03	0.7056	0.0097	17.3	3.0	-3.3	0.6
							4	-13.92	0.01	-4.00	0.02	0.6806	0.0073	25.4	2.4	-1.5	0.5
	5	19NOD06	25.7	30.0	20.0	845	7	-8.44	0.02	-7.44	0.03	0.7140	0.0099	14.7	3.0	-7.2	0.6
							6	-8.33	0.01	-6.63	0.07	0.6862	0.0059	23.5	2.0	-4.6	0.4
	6	19NOD07	27.6	31.9	22.1	647	10	-6.97	0.01	-6.85	0.03	0.7072	0.0092	16.8	2.8	-6.2	0.6
	5	19NOD08	27	31.3	21.3	720	10	-6.48	0.02	-8.86	0.13	0.7061	0.0121	17.1	3.7	-8.1	0.8
	7	19NOD09	27.3	31.6	21.9	655	7	-7.57	0.06	-7.36	0.07	0.7111	0.0099	15.6	3.0	-7.0	0.6
	8	20NOD01	27	31.5	20.9	869	7	-7.70	0.09	-5.43	0.07	0.0096	0.0099	22.2	3.2	-3.6	0.7
	9	20NOD03	26.8	31.0	21.4	723	8	-9.89	0.02	-8.59	0.06	0.7063	0.0093	17.1	2.9	-7.9	0.6
							4	-9.19	0.01	-7.07	0.03	0.6965	0.0073	20.2	2.3	-5.7	0.5
Early Miocene	3	19NAT13	N/A				8	-9.70	0.48	-4.13	0.90	0.6976	0.0121	19.8	3.8	-2.8	0.8
	3	19NAT01	N/A				5	-9.91	0.06	-1.63	0.05	0.6881	0.0091	22.9	3.0	0.3	0.6